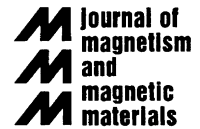




ELSEVIER

Journal of Magnetism and Magnetic Materials 246 (2002) 80–85



www.elsevier.com/locate/jmmm

## Direct experimental study of the exchange spring formation process

V.S. Gornakov<sup>a</sup>, V.I. Nikitenko<sup>a</sup>, A.J. Shapiro<sup>b</sup>, R.D. Shull<sup>b,\*</sup>,  
J. Samuel Jiang<sup>c</sup>, S.D. Bader<sup>c</sup>

<sup>a</sup>*Institute of Solid State Physics, Russian Academy of Sciences, Chernogolovka 142432, Russia*

<sup>b</sup>*National Institute of Standards and Technology, 100 Bureau Dr., Stop 8525, Gaithersburg, MD 20899 8525, USA*

<sup>c</sup>*Materials Science Division, Argonne National Laboratory, Argonne, IL 60439, USA*

Received 4 December 2001

---

### Abstract

The remagnetization of a soft ferromagnetic film exchange coupled with a high-coercivity ferromagnetic film is studied by a magneto-optic imaging technique. If the magnetic field is antiparallel to the macroscopic unidirectional in-plane anisotropy, the soft layer reverses via the formation of exchange springs consisting of subdomains with opposite spin twistings. However, if the field is instead rotated in-plane, remagnetization initially proceeds via formation of a single uniform exchange spring. Then, at a critical angle, the spring incoherently untwists, leading again to subdomains with opposite chirality. These phenomena are attributed to the influence of inhomogeneity in the unidirectional magnetic anisotropy. © 2002 Elsevier Science B.V. All rights reserved.

*PACS:* 75.70.Cn; 75.30.Et; 75.50.Kj

*Keywords:* Ferromagnetism; Exchange spring; Domain walls

---

Domain wall (DW) nucleation and motion are elementary steps in the remagnetization of a ferromagnet. The spin structures of various DWs and their dynamical properties can be described using the Landau–Lifshitz equation [1]. A DW can be viewed as a topologically stable exchange spring. Isotropic exchange interactions act to unwind the spring by orienting the spins parallel to each other. Anisotropic, relativistic interactions resist this action by anchoring the ends of the spring in the valleys of the potential energy

surface. The width  $\delta$  of a 180° ferromagnetic DW is determined by the ratio of the exchange  $A$  and magnetocrystalline anisotropy  $K$  such that  $\delta = \pi(A/K)^{1/2}$ , where  $\delta$  is typically tens to hundreds of nanometer. Remagnetization of bulk material essentially occurs via the motion of DW formed in nanoscale regions of the sample. Various methods have been developed to investigate DW displacement during the magnetization process. It has been established that the DW velocity depends on the effectiveness of energy transfer mechanisms via different excitations, including non-linear spin waves. In large external magnetic fields a transformation of the DW

---

\*Corresponding author.

*E-mail address:* shull@nist.gov (R.D. Shull).

structure can occur which gives rise to the formation of Bloch lines and points [1,2].

No prior experimental study of the exchange spring formation process exists because of the challenge of characterizing magnetic moments localized on the short length-scale of  $\delta$ . The features of the DW nucleation and growth are central to the fundamental physics and technology of new magnetic materials [3–17]. For example, in films consisting of thin layers (of thickness comparable to  $\delta$ ) of a soft ferromagnet exchange coupled to a hard ferromagnet, the remagnetization of the soft layer is determined exclusively by the exchange spring formation process [11–16]. This process is experimentally studied herein. It is found that exchange springs develop with opposite chirality due to incoherent spin rotations in adjacent areas during the magnetization reversal of the soft layer.

The sample consists of an epitaxial film of 50 nm of Fe(100) deposited by magnetron sputtering [15] onto 35 nm of Sm–Co grown on an MgO(001) substrate that is buffered with 20 nm of Cr(100). The sample was initially magnetized in a 7 T field along an in-plane Sm–Co easy axis in order to establish a unidirectional magnetic anisotropy in the soft layer. A hysteresis loop of the composite is shown in Fig. 1, measured in a field  $H$  oriented along the unidirectional anisotropy axis. From this loop one can see the discontinuous change due to the switching of the soft ferromagnetic layer at reversal fields  $<0.25$  T and the gradual switching of the hard SmCo layer at larger fields.

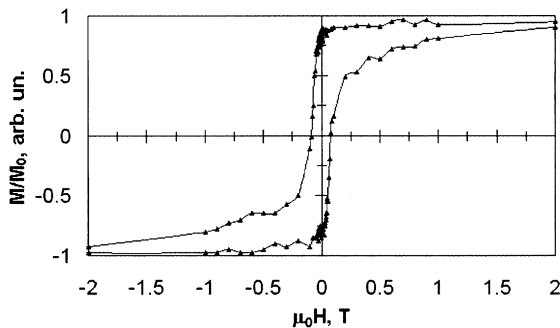


Fig. 1. Central part of a  $M$  vs.  $H$  hysteresis loop ( $-5 \text{ T} < H < +5 \text{ T}$ ) measured for the Fe/Sm–Co sample with  $H$  applied along the easy anisotropy axis.

The remagnetization processes in the bilayer were observed by means of visualizing the stray magnetic fields around the sample using a magneto-optic (MO) indicator film technique [17] with digital image processing. In this technique, a transparent, Bi-doped yttrium iron garnet indicator film is placed on top of the sample. In the absence of a magnetic field, the indicator magnetization is oriented in-plane, but it can deflect out of plane under the influence of perpendicular components of the stray field  $H_{\perp}$  around the sample. An MO image of the sample magnetic structure is observed in the reflected light using a polarizing microscope due to the double Faraday effect in the indicator film (and using slightly uncrossed polarizers at a small angle  $\beta$ ). For the bilayer investigated here, the total magnetic moment in the Fe layer is far greater than that of the Sm–Co, thereby causing a MO contrast which is dominated by the Fe layer.

The exchange spring formation is investigated on a sample for which a 300- $\mu\text{m}$  diameter hole was abrasively ground through the layers. The magnetic poles on opposite sides of the hole (Fig. 2) permit a determination of both the orientation and magnitude of the average magnetization ( $M$ ) of the surrounding region. The black and white colors of the MO image correspond to opposite signs of  $H_{\perp}$ . The magnitude of  $H_{\perp}$  is given by the intensity of the MO signal. For an in-plane  $M$  that is uniform in the vicinity of the hole, the MO contrast is at a maximum along the symmetry axis of its MO stray field image. This axis is parallel to  $M$  and delineated by the schematic compass needle shown in Fig. 2a. Photometric measurements of the MO signal intensity along this axis appear in Fig. 2b. Here the deviations from the mean intensity level (the gray background) of the MO signal at the left and right side edges of the hole are, respectively,  $I_L = I_0[\sin^2(\beta + \psi) - \sin^2 \beta]$  and  $I_R = I_0[\sin^2 \beta - \sin^2(\beta - \psi)]$ , where  $I_0$  is the intensity of the incident linearly polarized light and  $\psi$  is the Faraday rotation. For small  $\psi$  the average intensity  $I_A = (I_L + I_R)/2 \sim \psi \sim H_{\perp} \sim M$ . Thus, the average magnetization over the thickness of the bilayer is characterized by the value of  $I_A$  and by the angle  $\alpha$  of its rotation relative to the easy axis of magnetization. Changes in these values

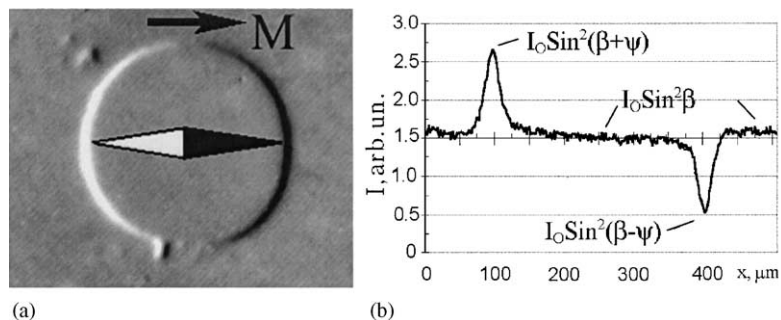


Fig. 2. (a) Magneto-optical image of a region of the sample containing a hole, and (b) intensity of the MO signal along the photometry line delineated by the schematic compass needle in (a).

during remagnetization of the soft layer provide a means for determining the spin distribution in that layer.

A technical point that must be addressed before proceeding is that the field that is applied in-plane can influence the MO signal because it can rotate the  $H_{\perp}$ -induced magnetic moments in the indicator film back into the film plane. This reduction in intensity of the useful MO signal can be accounted for by introducing a coefficient  $K^H = I_L^0/I_L^H$ , ( $I_L^0$  and  $I_L^H$  are the peak intensities measured at  $H = 0$  and  $H$ , respectively). The field dependence of  $K^H$  was measured in a separate experiment using positive applied fields (0–250 mT). In this field range,  $M$  is essentially constant (see Fig. 1) and, consequently, the intensity change of the MO signal depends only on the magnitude of  $H$ . The calibration experiment shows that  $K^H$  increases linearly with increasing  $H$ .

Our MO study of the exchange spring formation reveals significant disagreements with theoretical predictions [11–16]. We find, in particular, that the initiation and development of spin twisting do not lead to a uniform rotation of the in-plane magnetization of the soft layer during remagnetization. Uniform rotation is only observed when the field is oriented far away from the easy axis at some angle  $\varphi$ . An example of the magnetization reversal process and its characteristics for the  $\varphi = 10^\circ$  case is shown in Fig. 3. The easy anisotropy axis is indicated by the dotted line in Fig. 3a. As  $H$  is increased in the negative direction, the MO portrait of the stray fields around the hole changes (Fig. 3a). The symmetry axis rotates and the

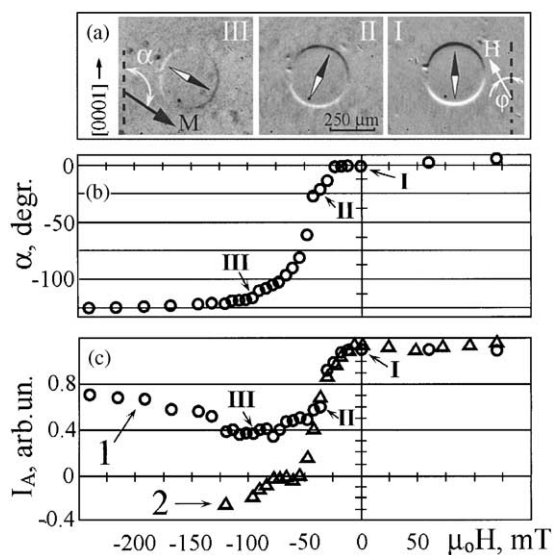


Fig. 3. (a) MO images of the sample region containing a hole, corresponding to points I–III in (b) and (c). Dotted lines indicate the easy magnetization direction. (b) Field dependence of the magnetization rotation angle  $\alpha$  for  $\varphi = 10^\circ$  and (c) the field dependence of the average intensity  $I_A$  of the magneto-optical signal for  $\varphi = 10^\circ$  (curve 1, circles) and  $\varphi = 0^\circ$  (curve 2, triangles).

intensity contrast decreases. This would appear to substantiate the prevalent conception that the remagnetization starts by the formation of a simple exchange spring due to the spins in the soft layer forming a spiral twist along a perpendicular to the interface [11–16]. However, the dependence of  $\alpha$  and  $I_A$  on  $H$  (Fig. 3b and c) cannot be explained by this simple model.

Note in Fig. 3b, that a critical field value of  $\sim -25$  mT is required before visible rotation of  $M$  occurs. Nevertheless, the value of  $I_A$  (Fig. 3c), measured for the first time in this study, decreases substantially (up to 15%) for  $|\mu_0 H| < 25$  mT in the reversed direction (while the rotation of  $M$  is essentially unobservable). Moreover, at  $\mu_0 H$  slightly in excess of  $-40$  mT, the sharp decrease in  $I_A$  ceases in spite of the fact that the rotation of  $M$  (see Fig. 3b) continues with increasing reversed field. The fact that the MO signal intensity does not scale with the rotation of  $M$  (for  $\varphi = 10^\circ$ ) proves the presence of non-uniformity in the spin-spiral formation during reversal of  $M$  in the soft layer.

Our data for the remagnetization with the field oriented antiparallel to the unidirectional anisotropy of the Fe layer ( $\varphi = 0^\circ$ ) reveal an even more paradoxical disagreement with the predictions of theory [11–16]. Curve 2 in Fig. 3c depicts the intensity change of the MO signal in this latter case. Upon field reversal,  $I_A$  initially drops to zero with increasing field magnitude to  $\sim -50$  mT. Further increase in  $|H|$  results in a contrast reversal followed by an increase in the MO intensity (indicated in Fig. 3c by an increase in the negative  $I_A$  values). However, the MO images do not reveal any rotation of the symmetry axis of the stray field distribution around the hole (and, hence, any rotation of the average in-plane magnetization of the sample) during remagnetization.

Comparison of curves 1 and 2 in Fig. 3c shows that during the first stage of remagnetization ( $\mu_0 H > -50$  mT) they essentially overlap. This indicates a decrease in the average in-plane magnetization of  $M$  despite the fact that in one case (for  $\varphi = 0^\circ$ ) rotation is not noted while in the other (for  $\varphi = 10^\circ$ ) it is. The fact that there is a reduction in the MO signal intensity without any discernable rotation of  $M$  (for  $\varphi = 0^\circ$ ) again proves that the magnetization reversal of the soft layer is non-uniform in plane. Such non-uniformity cannot be created by the formation of a simple exchange spring of a single chirality, but must derive from a more complex spin structure, presumably containing submicron-sized subdomains with different chirality (separated by Bloch lines).

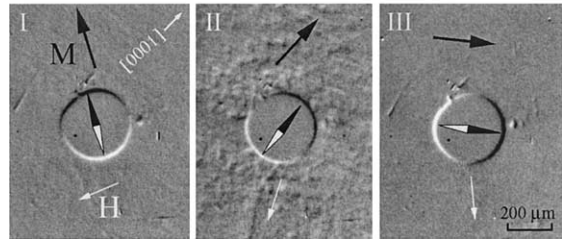
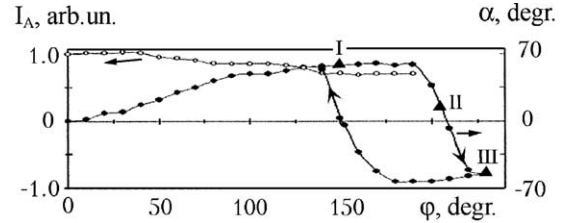


Fig. 4. Dependence of the average MO signal intensity  $I_A$  (open symbols) and the magnetization rotation angle  $\alpha$  (filled symbols) on the magnetic field rotation angle  $\varphi$  in the torque experiment. The bottom photographs show the sample region near the hole for  $\mu_0 H = 36$  mT corresponding to states I–III in the graph.

The presence of a complex exchange-spring structure is also confirmed by torque experiments (Fig. 4) wherein the amplitude of  $H$  is kept constant but its in-plane orientation is rotated. From the dependence of  $I_A(\varphi)$  and  $\alpha(\varphi)$  note that during the field rotation,  $M$  in stage I does not rotate in synchronization with the field, but lags behind; at  $\varphi = 150^\circ$   $M$  lags  $H$  by almost  $90^\circ$ . Simultaneously  $I_A$  decreases only slightly. Fig. 4 also shows that when  $\varphi$  reaches some critical value (here,  $\varphi_{cr} \approx 190^\circ$ ), the magnetization state of the sample becomes unstable; continued rotation of  $H$  in the same direction causes the rotation of  $M$  to change sign. During this instability the effective value  $I_A$  (and hence  $|M|$ ) continues to decrease (not shown in Fig. 4) and the MO image begins to exhibit magnetization ripples and micro-domains (Fig. 4b, Stage II). After the Stage II  $M$  reversal,  $|M|$  is similar to that at the beginning of the process, and  $M$  now leads  $H$  (Fig. 4, Stage III) with continued  $H$  rotation.

The relationship between  $I_A$  and  $\alpha$  (the magnitude and orientation of  $M$ ) is shown in Fig. 5 for both types of remagnetization. Curve 1 is for cycling  $H$  along a single axis (with  $\varphi = 10^\circ$ ), and

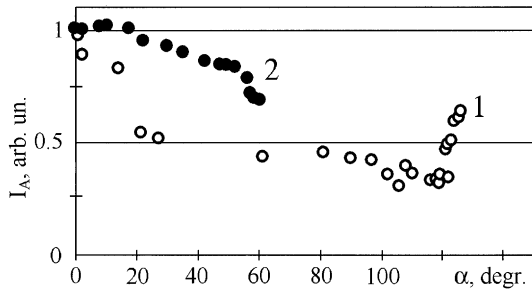


Fig. 5. Average MO signal intensity vs.  $M$  rotation angle ( $\alpha$ ) for uniaxial field reversal ( $\varphi = 10^\circ$ , curve 1, open symbols) and for iso-field rotation ( $\mu_0 H = 36$  mT, curve 2, filled symbols).

curve 2 is for rotating  $H$  ( $\mu_0 H = 36$  mT) about an axis perpendicular to the sample plane. In the first case, the magnetization rotation is accompanied by a sharp drop in  $I_A$ . In the second case, the MO signal intensity  $I_A$  is substantially less dependent on the rotation angle of  $M$ . At some critical angle  $\alpha$  ( $\sim 60^\circ$  in curve 2) determined by the magnitude of the applied field, the average magnetization over the bilayer thickness discontinuously changes to a new equilibrium direction (not indicated in Fig. 5). As mentioned above, the MO image shows an inhomogeneous spin structure during the discontinuous jump. This non-uniform MO contrast is not consistent with the simple picture of a single-chirality exchange spring. Instead, it shows that subdomains (spin spirals of opposite chirality) are created in a complex exchange spring structure.

The new spring structure with mixed chirality described above is a consequence of inhomogeneity in the direction of the unidirectional anisotropy. In general it is known that interfacial exchange coupling between a ferromagnet and a different magnetically ordered material breaks the magnetic symmetry of the system, causing the creation of a unidirectional exchange anisotropy in the ferromagnet. When an external field is antiparallel to this anisotropy direction, remagnetization proceeds by spin rotation in either the clockwise or counterclockwise sense. The uncertainty in spin twisting direction, however, is removed when  $H$  is oriented away from the anisotropy direction.

Real bilayer films inevitably contain lattice defects and interfacial imperfections. These entities

cause inhomogeneous changes in the orientation of the local unidirectional anisotropy axes across the whole sample. Their random deviations from the field direction results in incoherent spin rotation. Opposite chirality spin rotation occurs in different submicron areas that are too small to be directly resolved by the MO technique. In our sample, such opposing spin rotation structures in the Fe layer predominate when the field is oriented along the easy axis, as indicated by the  $M$  value dropping to zero and even changing sign (cf. curve 2, Fig. 3c). For this situation, no rotation of  $M$  is observed, consistent with there being only local spin rotations in different directions. Nano-domains are formed in this case, which are in essence subdomains in a Bloch-wall type exchange spring with different chiralities. The boundaries between them will be magnetic vortice-type line singularities (similar to a Bloch line in a domain wall [1]).

The overlapping of the  $I_A(H)$  curves for the  $\varphi = 10^\circ$  and  $0^\circ$  experiments (curves 1 and 2, respectively, in Fig. 3c) for  $\mu_0 H > -40$  mT show that even for  $\varphi = 10^\circ$ , there exist spin rotations in opposite directions in different micro-regions of the Fe-layer. We conclude this because, as described above, we know such opposite spin rotations occur in the  $\varphi = 0^\circ$  case. The stabilization and subsequent increase in  $M$  (Fig. 3c, curve 1) with increasing (negative) magnitude of  $H$  (for  $\mu_0 H < -50$  mT) in the  $\varphi = 10^\circ$  experiment may be due to the following two effects. Firstly, the loss in stability can cause a subsequent change in the spin twisting direction of a number of nano-domains in which the spins were initially twisted in the opposite direction. And secondly,  $M$  can increase because of increasing alignment of the spins furthest away from the pinned interface, near the free surface of the soft layer, in the twisted spin arrangement as  $H$  increases.

The remagnetization of the bilayer film under field rotation confirms that incoherent behavior occurs when it is in an unstable condition (Fig. 4). Fig. 4 (stage II) shows an inversion of the rotation direction of  $M$  as the spin system stability is lost. These results, and the appearance of magnetization ripples in the MO image, can only be explained by the nucleation and growth of

exchange springs (of the Bloch-wall type) with local spin twisting directions opposite to the initial twisting.

Fig. 5 shows a comparison of the  $I_A$  values for the rotation of  $M$  via field reversal (curve 1) and field rotation (curve 2). It is obvious that the average total magnetizations are not equal at the same rotation angle. In curve 2 the higher value of  $M$  is caused by the rotation of almost all the spins in the Fe layer. While in curve 1, where  $H$  is oriented opposite, or almost opposite, to the induced unidirectional anisotropy in the Fe layer, one part of the spin system twists clockwise while the other twists counterclockwise. This phenomenon is caused by significant inhomogeneity of the magnetic anisotropy direction at the bilayer interface. The magnitude of the inhomogeneity in the easy axis orientation can be estimated from Fig. 4. It is approximately equal to the width of the stage II steps on the  $I_A(\varphi)$  curves.

In conclusion, it is shown that remagnetization opposite to the macroscopic unidirectional anisotropy of a soft ferromagnetic thin film exchange-coupled to a high-coercivity layer is not characterized by uniform spin rotation along the whole interface. This means that the spin configuration during remagnetization is not that of a simple, exchange spring of a single chirality. Instead, it is comprised of adjacent local spin-spirals with opposite chiralities. The local sign of the rotation is determined by the direction of the local unidirectional anisotropy (correlated with crystal lattice misorientations and imperfections) relative to the direction of the remagnetizing field.

Work at Argonne was supported by the US Department of Energy, Division of Basic Energy Sciences-Material Sciences under contract No. W-31-109-ENG-38.

## References

- [1] A.P. Malozemoff, J.S. Slonczewski, *Magnetic Domain Walls in Bubble Materials*, Academic, New York, 1979; A. Hubert, R. Schäfer, *Magnetic Domains*, Springer, Berlin, 1998.
- [2] V.I. Nikitenko, et al., in: *Proceedings of the Third International Conference on Physics of Magnetic Materials*, World Scientific, Singapore, 1987, p. 122; L.M. Dedukh, V.S. Gornakov, V.I. Nikitenko, *J. de Phys.* 49 (1988) C8-1865.
- [3] W.H. Meiklejohn, C.P. Bean, *Phys. Rev.* 102 (1956) 1413; W.H. Meiklejohn, C.P. Bean, *Phys. Rev.* 105 (1957) 904.
- [4] A.E. Berkowitz, K. Takano, *J. Magn. Magn. Mater.* 200 (1999) 552; J. Nogues, I.K. Shuller, *J. Magn. Magn. Mater.* 192 (1999) 203.
- [5] V.I. Nikitenko, et al., *Phys. Rev. Lett.* 84 (2000) 765.
- [6] P. Grünberg, et al., *Phys. Rev. Lett.* 57 (1986) 2442.
- [7] M.N. Baibich, et al., *Phys. Rev. Lett.* 61 (1988) 2472; A. Barthelemy, et al., *Handbook of Magnetic Materials*, Vol. 12, North-Holland, Amsterdam, 1999.
- [8] S.S.P. Parkin, et al., *Phys. Rev. Lett.* 64 (1990) 2304.
- [9] J. Unguris, et al., *Phys. Rev. Lett.* 67 (1991) 140.
- [10] N.J. Gökenmeijer, et al., *Phys. Rev. Lett.* 79 (1997) 4270.
- [11] E. Kneller, R. Hawig, *IEEE Trans. Magn.* 27 (1991) 3588.
- [12] E.E. Fullerton, et al., *Phys. Rev. B* 58 (1998) 12193.
- [13] J. Astalos, R.E. Camley, *Phys. Rev. B* 58 (1998) 8646.
- [14] K. Mibu, et al., *Phys. Rev. B* 58 (1998) 6442.
- [15] E.E. Fullerton, et al., *J. Magn. Magn. Mater.* 200 (1999) 392.
- [16] J.S. Jiang, et al., *IEEE Trans. Magn.* 35 (1999) 3229.
- [17] V.I. Nikitenko, et al., *Phys. Rev. B* 57 (1998) R8111.